Implications of Proprotein Convertases in Ovarian Cancer Cell Proliferation and Tumor Progression: Insights for PACE4 as a Therapeutic Target[1]

Rémi Longuespée*,[†], Frédéric Couture[†], Christine Levesque[†], Anna Kwiatkowska[†], Roxane Desjardins[†], Sandra Gagnon[†], Daniele Vergara*,[‡], Michelle Maffia[‡], Isabelle Fournier*, Michel Salzet*, and Robert Day[†]

*MALDI Imaging Team, Laboratoire de Spectrométrie de Masse Biologique Fondamentale et Appliquée, Université Nord de France, Cité Scientifique, Université de Lille 1, Villeneuve D'Ascq, France; [†]Faculté de Médecine et des Sciences de la Santé, Institut de Pharmacologie de Sherbrooke et Département de chirurgie et service d'urologie, Université de Sherbrooke, Sherbrooke, Canada; [‡]Laboratory of Clinical Proteomic, "Giovanni Paolo II" Hospital, ASL-Lecce, Italy

Abstract

Proprotein convertases are a family of kexin-like serine proteases that process proteins at single and multiple basic residues. Among the predicted and identified PC substrates, an increasing number of proteins having functions in cancer progression indicate that PCs may be potential targets for antineoplastic drugs. In support of this notion, we identified PACE4 as a vital PC involved in prostate cancer proliferation and progression, contrasting with the other co-expressed PCs. The aim of the present study was to test the importance of PCs in ovarian cancer cell proliferation and tumor progression. Based on tissue-expression profiles, furin, PACE4, PC5/6 and PC7 all displayed increased expression in primary tumor, ascites cells and metastases. These PCs were also expressed in variable levels in three model ovarian cell lines tested, namely SKOV3, CAOV3 and OVCAR3 cells. Since SKOV3 cells closely represented the PC expression profile of ovarian cancer cells, we chose them to test the effects of PC silencing using stable gene-silencing shRNA strategy to generate knockdown SKOV3 cells for each expressed PC. *In vitro* and *in vivo* assays confirmed the role of PACE4 in the sustainment of SKOV3 cell proliferation, which was not observed with the other three PCs. We also tested PACE4 peptide inhibitors on all three cell lines and observed consequent reduced cell proliferation which was correlated with PACE4 expression. Overall, these data support a role of PACE4 in promoting cell proliferation in ovarian cancer and provides further evidence for PACE4 as a potential therapeutic target.

Translational Oncology (2014) 7, 410–419

Introduction

Ovarian cancer is characterized by a multisequential process, which involves multiple gains in cell functions, conferring to the transformed cells the capacity for increased proliferation and metastasis. These changes are partially mediated by alterations in genetic and protein expression levels, thus allowing for increased cell division, tissue invasion, and cell adhesion as well as colonization in new microenvironments [1]. Among the newest recognized molecular actors involved, the proprotein convertases (PCs) are important in cancer progression through their processing and activation of cancer-associated proteins [2]. Although numerous cancer-associated proteins are likely involved, proprotein processing can still be considered as a limiting step that cancer cells require to gain their full self-sustaining capabilities [2].

PCs are a family of serine proteases responsible for protein processing within the secretory pathway. Nine family members have been identified in mammalian cells, including furin, PACE4, PC1/3, PC2, PC4, PC5/6, PC7, PCSK9, and substilisin-kexin isoenzyme 1 (SKI-1) [3]. Only the first seven PCs cleave their substrates in the C terminus at the R-X-X-R consensus motif. Among these PCs, furin is ubiquitous, whereas PC1/3 and PC2 are categorized as endocrine specific. Despite the well-accepted identity of PC substrates, which are largely known from their consensus cleavage site in their primary sequences, the cleavage specificity among the enzyme family is still fragmentary and remains difficult to establish because the PC catalytic domain is highly conserved [4].

The role of PCs has been described in breast cancer [5], head and neck cancer [6], and recently prostate cancer [7]. Various PC substrates have recognized roles in cell growth, tumor angiogenesis, invasion, and metastasis, including secreted growth factors, matrix metalloproteinases, and adhesion molecules [8]. The implication of the different PCs in ovarian cancer is controversial, as PACE4, in contrast to prostate cancer studies, has been reported to be epigenetically silenced [9] and furin to be highly expressed in ovarian cancer cells [10]. These data contrast with those published in open sources such as Oncomine databases (Compendia Bioscience, Ann Arbor, MI) where PACE4 expression varies significantly according to data sets but tends to increase in tumor tissues, just like furin and PC7. Thus, the functional roles and redundancies of PCs in ovarian cancer context remain unclear.

In the present study, we used molecular silencing [i.e., lentivirus-delivered small hairpin RNAs (shRNAs)] to knock down each endogenously coexpressed PC in the SKOV3 cell line and then test for cell proliferation and tumor progression response. SKOV3 cells are the most studied models for serous ovarian cancer and display strong expression of furin, PACE4, PC5/6, and PC7, similar to ovarian cancer tissues and metastases. Our molecular silencing approach method is highly specific and permits a better distinction in regards to PC functional redundancy. We also examined the effects of our recently developed specific PACE4 inhibitor, namely, the Multi-Leu (ML) peptide and some peptidomimetic analogs in SKOV3 cells, as well as two other cell lines, OVCAR3 and CAOV3 cells. The sum of our data confirms that PACE4, and no other PCs, has an important role in ovarian cancer cell proliferation and further suggests that PACE4 is a potential therapeutic target.

Materials and Methods

Tissue Sample Collection and Reverse Transcription–Polymerase Chain Reaction Analysis

Tissues were obtained from Lecce, Italy, with institutional review board approval by the Human Bioethic Center of University of Salento and "Vito Fazzi" Hospital, from patients undergoing ovarian tumor resection. All patients provided written informed consent. Samples were collected at the time of the surgery, immediately frozen at − 50°C, in isopentane, and stored at − 80°C until analysis. Total cellular RNA was isolated by illustra triplePrep extraction kit (GE Healthcare) following the manufacturer's instruction and immediately used. Total RNA (1 μg) was reverse transcribed into cDNA using the M-MLV reverse transcriptase enzyme (Invitrogen, Carlsbad, CA). Polymerase chain reaction (PCR) was carried out using the following conditions: denaturation at 95°C for 60 seconds, annealing at 60°C for 60 seconds, and extension at 72°C for 60 seconds. PCR products were visualized after migration on a 1% agarose gel containing 0.25 μg/ml ethidium bromide and visualized under UV light. Primers used for reverse transcription–PCR (RT-PCR) are given as follows: Glyceraldehyde 3-phosphate dehydrogenase (GAPDH), forward—5'-GCATGGCCTTCCGTGTCCC-3' and reverse—5'-CAATGCCAGCCCCAGCGTCA-3'; PACE4, forward—5'-CTATGGATTTGGTTTGGTGGAC-3' and reverse—5'-AGGCTCCATTCTTTCAACTTCC-3'; PC5/6, forward—5'-GATGCAAGCAACGAGAACAA-3' and reverse—5'-GCAGTGGTCTTTGCTCCTTC-3'; PC7, forward—5'-ATCATTGTCTTCACAGCC-3' and reverse—5'-AAGCCTGTAGGTCCCTC-3'; and furin, forward—5'-TATGGCTACGGGCTTTTGG-3' and reverse—5'-TTCGCTGGTGTTTTCAATCTCT-3'.

Cell Culture

All cell culture media and FBS were obtained from Wisent Bioproducts (Saint-Bruno, Québec). SKOV3 and CAOV3 cells were cultured in Dulbecco's modified Eagle's medium–F12 medium with 10% FBS. OVCAR3 cells were cultivated in RPMI 1640 with 20% FBS and 10 mg/l insulin (Wisent). HEK293FT cells (Invitrogen) were grown in Dulbecco's modified Eagle's medium containing 10% FBS, 6 mM glutamine, and 500 μg/ml G418. All cell lines were cultured at 37°C in a water-saturated atmosphere with 5% CO_2.

Lentiviral Particle Production and shRNA Transduction

MISSION RNAi pLKO.1-puro vectors for each PC were purchased from Sigma-Aldrich (St Louis, MO) as described in [11,12]. Lentivirus particles containing these shRNAs were produced in the HEK293FT cell line. shRNA sequences are listed as follows with their Sigma The RNAi Consortium (TRC) number: furin—CCTGTCCCTCTAAAGCAATAA (TRC: TRCN0000075238), PACE4—CCTGGAAGATTACTACCATTT (TRC: TRCN0000075250), PC5/6—TTTCGGAAATTCATTGGTTGGT (TRC: TRCN0000051179), and PC7—GCACTATCAGATCAATGACAT (TRCN0000072394). SKOV3 cells were infected with the virus-containing media and selected with 3 μg/ml puromycin (the lowest concentration able to eliminate untransfected cells) 2 days after infection. Knockdown cell lines were further cultured under selection conditions. shRNA sequences were selected on the basis of results shown by Couture et al. [11].

Reverse Transcription– and Real-Time Polymerase Chain Reaction

Total RNA was extracted from cell pellet obtained following trypsin treatment using the Qiagen RNA isolation kit (Qiagen, Valencia, CA), and quality was assessed using RNA Nano Chips using an Agilent Bioanalyzer (Agilent Technologies, Palo Alto, CA). Relative expression levels were calculated using β-actin as a reference gene like in [11]. Experiments were performed at least three times in duplicate (n = 3). Primers used are those defined in [11].

XTT Cell Proliferation Assay

The XTT Cell Proliferation Kit II (Roche Applied Science, Indianapolis, IN) was used following the manufacturer's instructions. This assay is a nonwash colorimetric assay for cell proliferation and cell viability measurement. For this assay, an 2,3-Bis(2-methoxy-4-nitro-5-sulfophenyl)-2H-tetrazolium-5-carboxanilide (XTT) tetrazolium salt is reduced by dehydrogenase enzymes in metabolically active cells in a soluble formazan, allowing direct measure of metabolic activity without removing the media from the plate. Briefly, 1000 cells of each cell line were plated onto 96-well plates in 100 μl of complete culture media. Every following 24 hours until 96 hours of growth, XTT reagent was added to each well, and the plates were incubated for 5 hours. Absorbance values were measured at 490 nm with a reference at 690 nm in a microplate reader (SpectraMax 190; Molecular Devices, Sunnyvale, CA). Experiments were performed in five replicates for each cell line at least five times ($n = 5$). Means were reported for the 24-hour absorbance value for each cell line.

Clonogenicity Assays

A clonogenicity assay was performed by plating 400 cells of each cell line in six-well plates with 2 ml of complete media for 15 days. Media were then discarded, and 1 ml of 5 mg/ml methylene blue with 50% methanol was added. After 10 minutes, wells were rinsed carefully with distilled water and dried to allow for the manual counting of stained colonies. Only colonies with >40 cells were considered.

Human Tumor Xenograft Models

Exponentially growing cells (2×10^6) were collected and injected subcutaneously in shoulders and flanks of five to six female Nu/Nu mice (Charles River, Saint-Bruno, Québec) for each cell line. Tumor volumes were determined using a digital caliper three times per week using the following formula: tumor volume = $(L \times W^2) \times \pi/6$, where L is the tumor length and W is the tumor width. At the end of the experiment, tumors were excised and fixed in formalin before paraffin embedding for further immunohistochemistry (IHC).

IHC of Tissue Markers in Xenograft Model Tumors

IHC were performed on 5-μm tumor sections in the Department of Pathology of the Centre Hospitalier Universitaire de Sherbrooke, Québec (CHUS) (Sherbrooke) using a standard streptavidin-biotin-peroxidase immunostaining procedure with a Ventana NexES auto-stainer and the solvent-resistant DAB Map detection kit (Ventana Medical Systems, Tucson, AZ) using ready-to-use solutions (Ki67 and E-cadherin) purchased from Dako, Burlington, Ontario, Canada.

Ki67-positive cells were manually counted in up to five × 400 light microscope representative fields per tumor (containing an average of 150 cells). Total counts were reported as total cell number per field. E-cadherin protein levels were quantified using the yellow channel of a cyan, magenta, yellow, key (CMYK) color model with pictures taken with a Super Coolscan 9000 scanner (Nikon, Tokyo, Japan) using Fiji software (Open Source) [13], and quantification was performed using Image-Pro software (Media Cybernetics, Bethesda, MD). To avoid quantification of any nontumoral area (e.g., skin and fat), the xenograft sections were counterstained using hematoxylin and eosin in addition to staining the estrogen receptor, a positive marker of SKOV3 cells. Pictures with × 100 and × 400 magnifications were acquired using an Axioskop 2 phase-contrast microscope (Carl Zeiss, Thornwood, NY) and processed using Image-Pro software.

Peptide and Peptidomimetic Inhibitors

All compounds used in this study were prepared as previously described [14].

Growth Inhibition Assay

3-(4,5-dimethylthiazol-2-yl)-2,5-diphenyltetrazolium bromide cell proliferation assays were performed as described previously [15]. Briefly, cells were plated onto 96-well poly-(L)-lysine–coated plates at a density of either 1500 SKOV3 or 4500 OVCAR3 or 3000 CAOV3 cells per well. After 24 hours of incubation, the media were changed, and peptides were added to fresh complete media. The metabolic activity was monitored as described previously by Levesque et al. [15].

Statistical Analysis

All experiments were repeated at least five times, and the results were expressed as means ± SEM. Statistical analysis was done using Student's t test to calculate P values and determine statistical significance.

Results

PC Expression Pattern in Ovarian Cancer Stages and Cell Models

On the basis of the data available in Oncomine databases, PCs trend toward a global overexpression in ovarian cancer when compared to normal tissues. We first decided to investigate this trend in PC expression using RT-PCR in tissue samples originating from normal ovaries, ovarian tumors, ascitic cells, and distant metastases. As shown in Figure 1A, furin, PACE4, PC5/6, and PC7
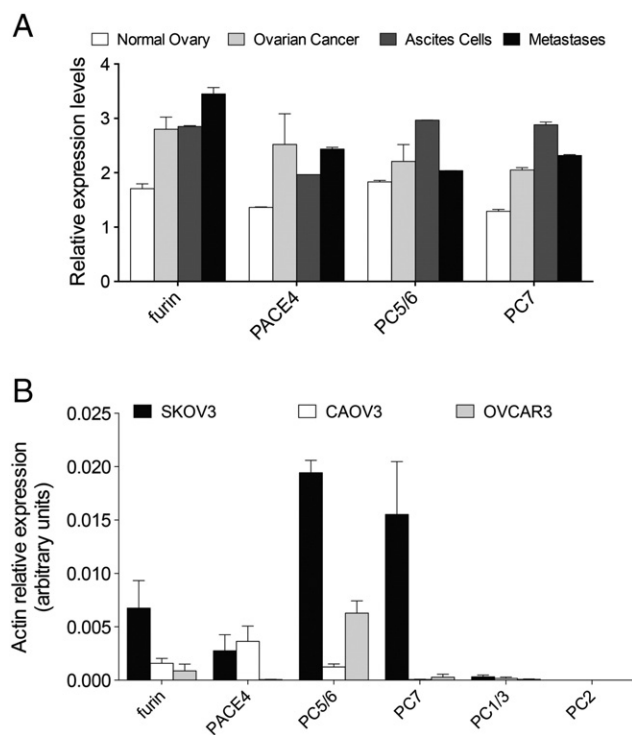
Figure 1. PC expression profile among ovarian cancer tissues and cell lines. (A) RT-PCR evaluation of the PCs furin, PACE4, PC5/6, and PC7 in normal ovaries ($n = 4$), ovarian primary tumors ($n = 4$), ascitic cells ($n = 2$), and metastases ($n = 2$) is shown. (B) RT-qPCR analyses of relative mRNA levels for each PC member in the SKOV3, CAOV3, and OVCAR3 cells ($n = 3$) are shown. Data are means ± SEM of experiments performed in duplicate.

were all upregulated in the cancerous stages (primary tumor, ascites, and metastases), confirming the Oncomine databases.

The expression of endogenous PCs was further examined in well-known ovarian cancer cell models, including SKOV3, OVCAR3, and CAOV3. Reverse transcription– and real-time PCR (RT-qPCR) analyses were performed for each PC, and the expression was normalized using β-actin mRNA levels. Results are presented in Figure 1B. Furin is expressed in all analyzed cell lines, as expected. SKOV3 cells also expressed high levels of PACE4, PC5/6, and PC7, when compared to other cell lines. In addition to furin, OVCAR3 cells expressed only PC5/6 and PC7, whereas CAOV3 expressed only PACE4 and PC5/6.

Down-Regulation of Endogenously Expressed PCs

Because the overall expression of furin, PACE4, PC5/6, and PC7 is increased in ovarian cancer tissues compared to normal tissues from Oncomine databases and our analysis further validated this result (Figure 1A), we chose SKOV3 cell line as the best model to examine the role of each PC in cell proliferation and tumor progression, because this cell line coexpresses high levels of these PCs. A lentiviral delivery strategy was used to generate stable shRNA-expressing cells for each of these PCs [11,12]. Consistent with the previously determined gene silencing efficiency for human PC shRNA sets [11], the two most efficient sequences were used to knock down these PCs

in SKOV3 cells, and the most efficiently silenced cell line was further used for the cell-based assays. Knockdown efficiency was assessed by RT-qPCR using the nontarget (NT) shRNA-expressing cells as a control. The results are presented in Figure 2. The residual expression in the selected knockdown cells was 16% for shfurin, 28% for shPACE4, 4% for shPC5/6, and 37% for shPC7.

PC7 and PACE4 Knockdowns Reduce the Cell Proliferation and Colony Formation of SKOV3 Cells

XTT cell proliferation assays were used to determine the importance of each PC in cell growth [12,16]. Cell growth was monitored for 96 hours and plotted using the respective increase of absorbance relative to each starting value at 24 hours. The results are presented in Figure 3A. PACE4 and PC7 knockdown cells exhibited a significantly reduced growth rate compared to the NT control cell line. The knockdown cell lines displayed an overall reduction of 35% for shPC7 and 34% for shPACE4 relative to the control cells. Interestingly, the growth rate of furin knockdown cells remained unchanged compared to the control cells, whereas PC5/6 knockdown only slightly affected cell growth (20% reduction of proliferation compared to NT).

Cell clonogenicity potential, which is defined as the capacity of a single cell to form a colony, was further assessed because it involves cell growth factor self-sufficiency, an important facet of cancer cell
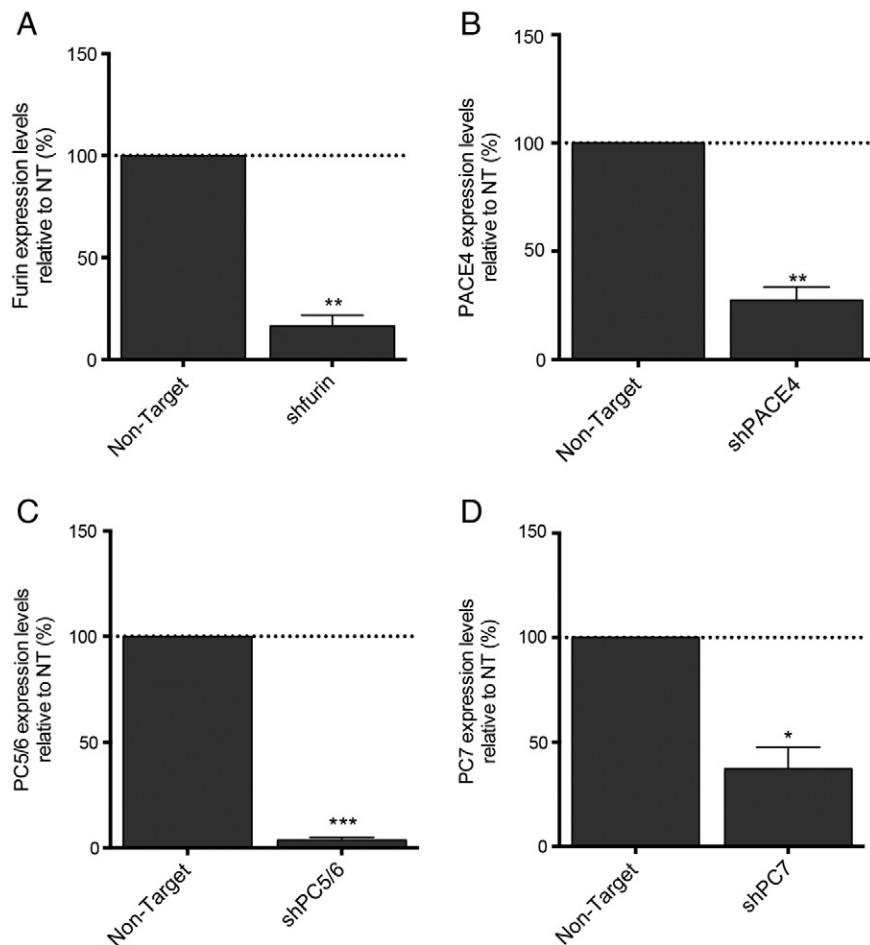

Figure 2. PC expression profile in SKOV3 cells. Knockdown levels for furin (A), PACE4 (B), PC5/6 (C) and PC7 (D) were assessed by RT-qPCR following the generation of two stable knockdown cell lines per PC. Data are means ± SEM of at least three independent experiments ($n = 3$) performed in duplicate. *$P < .05$ and **$P < .01$.
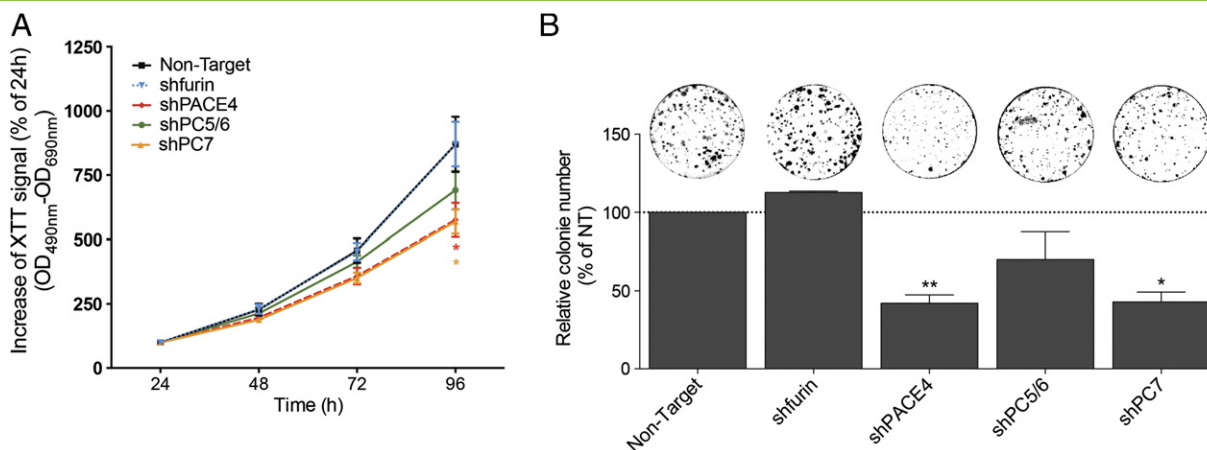
Figure 3. *In vitro* cell growth assay. (A) XTT assays were performed for each selected PC knockdown cell line. Colorimetric measures (OD_{490}–OD_{690} nm) were taken at 24, 48, 72, and 96 hours after seeding 1×10^3 cells per well. Growth was monitored as percentage of the 24-hour value. Data are means ± SEM of at least three independent experiments ($n = 3$) performed in duplicate. *$P < .05$. (B) Colony formation assay was performed on seeding 200 cells in six-well plates, which were allowed to grow 15 days before being stained and manually counted. Representative colonies are shown. Data are means ± SEM of at least three independent experiments ($n = 3$) performed in duplicate. *$P < .05$ and **$P < .01$.

proliferation. Cells were seeded at low density (400 cells in six-well plates) and allowed 10 days to form colonies, which were stained and manually counted. The results are presented in Figure 3B. Consistent with the proliferation assays, PACE4 and PC7 knockdown cells formed significantly fewer colonies than the NT control cells (42% and 40%, respectively), and no significant changes were observed for the furin and PC5/6 knockdown cells.

PACE4 Gene Silencing Prevents the Xenograft Progression in Athymic Nude Mice

As the cell culture environment has the obvious limitations of *in vitro* experiments, the physiological context was then considered in an effort to validate the obtained cell proliferation and clonogenicity results. Each knockdown cell line was subcutaneously xenografted on athymic nude mice, and tumor volumes were monitored over time. Mean tumor volumes were determined and plotted (Figure 4, A and B). As previously reported, a tumor latency phase was observed before the tumors reached an exponential growth phase [17]. Interestingly, in contrast with the results from the *in vitro* assays, only the PACE4 knockdown cell–derived xenografts had a statistically significant lower growth rate when compared to control NT cells (37% overall reduction of tumor sizes). Moreover, the PC7 knockdown xenograft behavior was strikingly different when compared to the *in vitro* assay as their tumor growth rates were significantly higher than the growth rates of the control tumors (29% overall increase in tumor sizes). Consistent with the *in vitro* assays, the growth rates of both furin and PC5/6 knockdown tumors remained unchanged.

At the end of the experiment, the mice were killed, and tumors were excised and weighed. The average tumor weights are reported in Figure 4C. Consistent with their growth rates, PC7 knockdown–derived tumors had significantly higher weights (250 ± 30 mg) than the PACE4 knockdown–derived tumors, which were significantly lower (100 ± 20 mg) when compared to the control tumors (170 ± 20 mg). No significant changes in tumor weights were observed for the furin and PC5/6 knockdowns (averages of 170 and 150 mg, respectively).

Molecular Markers Suggest that the Proliferation Index Is Decreased in PACE4 Knockdown Cell–Derived Xenografts and that PC7 Acts as a Tumor Growth Restrictor In Vivo

Molecular markers were analyzed by IHC in xenografts to evaluate the biologic processes of proliferation that might clarify the growth disparity between *in vitro* and *in vivo* conditions. Analyses were performed on excised xenograft sections with the Ki67 proliferation marker, which stains nuclei and allows the proliferating cells to be discriminated. Thus, the determination of Ki67-positive nuclei provided insights supporting tumor growth behavior. The results presented in Figure 5A indicated that cell proliferation indexes among the PC knockdown cell–derived xenografts were equal compared to the NT controls with the exception of PACE4 knockdown cell–derived xenografts, which had a significantly lower index (70%), and furin knockdown cell–derived xenografts, where only a slight but statistically significant difference was observed (87%). These observations supported the growth phenotype observed for PACE4-silenced cells and tumors.

E-cadherin has a dual role in the different phases of ovarian cancer metastasis [18]. E-cadherin has antiproliferative effects on cells before they undergo epithelial-to-mesenchymal transition in many types of cancers, including epithelial ovarian cancers (EOCs) [19]. IHC were performed against E-cadherin on the xenograft sections, and relative protein levels were quantified (Figure 5, B and C). Interestingly, significantly higher E-cadherin levels were observed in the PC7-silenced xenografts (176%) without significant variation for the other xenograft types assayed when compared to controls.

PACE4 Inhibitors Display PACE4-Dependent Growth Inhibition Properties when Applied on Ovarian Cancer Cell Models

To further test the effect of PACE4 inhibition, we examined the pharmacological effect of the previously described PACE4 inhibitor ML peptide and its peptidomimetic analogs on the proliferation of the three model cell lines. This analysis takes into account the variable levels of PACE4 expression. The PACE4 inhibitor Ac-LLLLRVKR-NH$_2$ [15] and its analog Ac-[DLeu]LLLRVKR-NH$_2$ [14] have inhibitory constants (K_i) in the low nanomolar range against PACE4
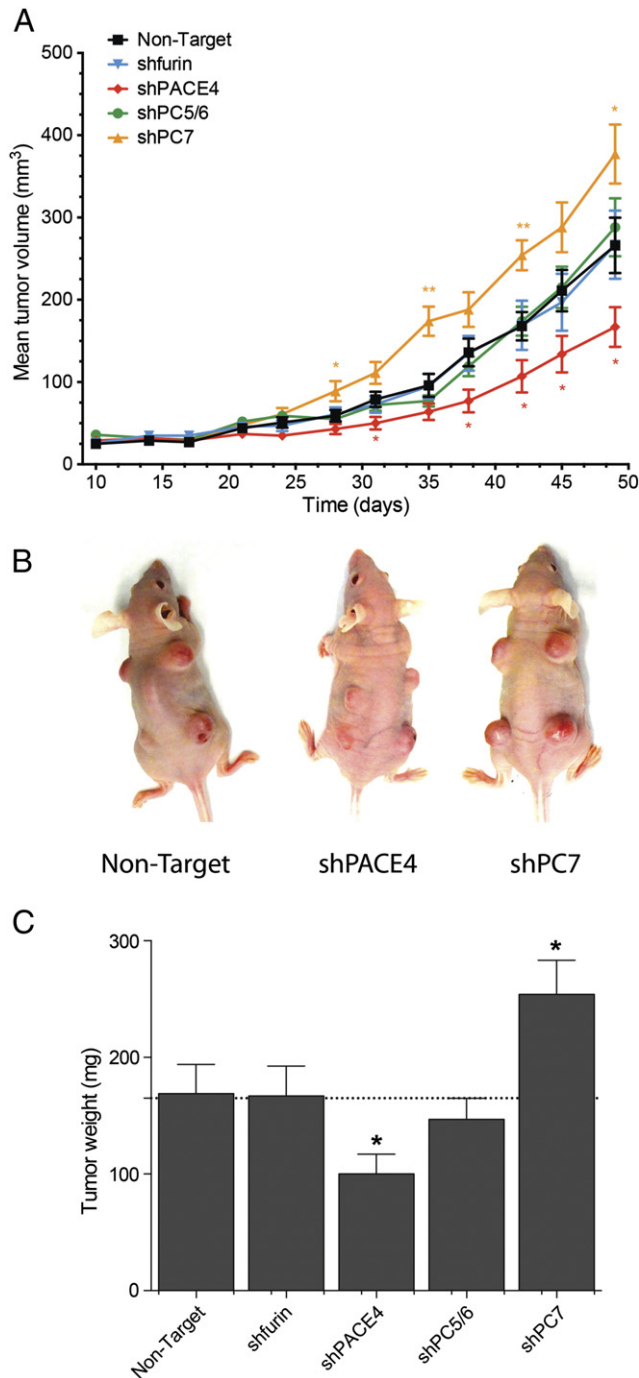
Figure 4. *In vivo* xenograft formation assay. (A) Exponentially growing cells (2×10^6) were injected subcutaneously in athymic nude mice (four sites per mouse; five to six mice per group). Tumor volumes were monitored regularly. Data are means ± SEM of all tumor volumes per group. *$P < .05$ and **$P < .01$. (B) Pictures of representative xenografted mice show tumor size differences. (C) On day 50, tumors were excised after mice killing, and tumor weights were measured. Data are means ± SEM of all tumor weights per group. *$P < .05$.

(K_i's = 20 and 24 nM, respectively). Ac-LLLLRVKR-NH$_2$ and Ac-[DLeu]LLLRVKR-NH$_2$ displayed half-maximal growth inhibition concentration (IC$_{50}$) in the mid-micromolar range in the PACE4-positive SKOV3 (320 and 220 μM, respectively) and CAOV3 (450

and 220 μM, respectively; Figure 6). A more potent analog, which has the 4-amidinobenzylamide (Amba), an arginine mimetic, at its C terminus; Ac-LLLLRVK-Amba is almost 10-fold more potent for PACE4 (K_i = 3 nM) [14]) and had lower IC$_{50}$s (140 and 70, respectively) for the SKOV3 and CAOV3 cells). When applied on the PACE4-negative OVCAR3 cells, the peptide displayed no significant growth inhibition with concentrations up to 500 μM (concentration limit due to solubility properties). Additionally, a negative control peptide lacking the critical R residue at the C terminus, Ac-LLLLRVKA-NH$_2$, did not exhibit antiproliferative properties in PACE4-expressing cell lines. These data support PACE4 dependence in ovarian cancer for sustained proliferation.

Discussion

According to American and European statistics, ovarian cancer is the most lethal of all gynecological cancers. The latest projection for 2013 in the United States reports that approximately 22,240 women received a new diagnosis of ovarian cancer, leading to 14,030 deaths [20]. In Europe, more than 65,500 new cases were estimated in 2012, leading to 42,700 deaths [21]. This affliction is commonly called the "silent killer" because its evolution does not indicate any clear symptoms [22].

PCs are essential for physiological and pathologic cellular processes. These important enzymes have critical roles in neoplasm formation, progression, and metastasis through the processing of a variety of oncoproteins, such as growth factors and their receptors, as well as membrane and extracellular matrix proproteins involved in tumor progression [23,3]. The prediction of their substrate cleavage specificities is hindered due to the highly conserved nature of their catalytic sites and observed redundancies using *in vitro* assays. Nonetheless, the ability to discriminate the distinct and redundant functions that drive cancer-related aspects of a given cancer type remains possible within an *in vivo* context, because PCs have different tissue and intracellular localizations. Because we believe that targeting PCs upstream of converging cancer pathways could attenuate the aggressiveness of cancer cells with limited physiological drawbacks on normal cells [3], this is of great relevance for the development of targeted therapeutic strategies. The question remains as to which PCs need to be targeted, to provide the best chances of a beneficial effect.

To evaluate the relative cancer-sustaining functions of each PC in ovarian cancer, we used a gene-silencing method to generate individual cell lines, each lacking an endogenously expressed PC member. Because pharmacological compounds selectively targeting each member of the PC family are limited, this method represents the best option allowing for the direct comparison of the implication of PCs in cell proliferation both *in vitro* and *in vivo* [12]. On the basis of the observation that ovarian tumor tissues, and also ascites cells and metastases, display variable levels of PC expression (Oncomine databases; Figure 1*A*), we opted for the SKOV3 cells to explore the relative implication of each PCs, as they coexpressed the four relevant PCs: furin, PACE4, PC5/6, and PC7 (see Figure 1*B*).

Using *in vitro* proliferation assays, we observed the effects of PACE4 and PC7 molecular silencing through proliferation and colony formation assays in these cells. *In vivo* xenograft formation assays supported the phenotype observed with PACE4-silenced cells; however, the observations in this assay contrasted with PC7 knockdown cells, which displayed unexpected increased tumor progression capabilities when implanted in athymic nude mice, contrasting with the *in vitro* proliferation assays. Although we found a
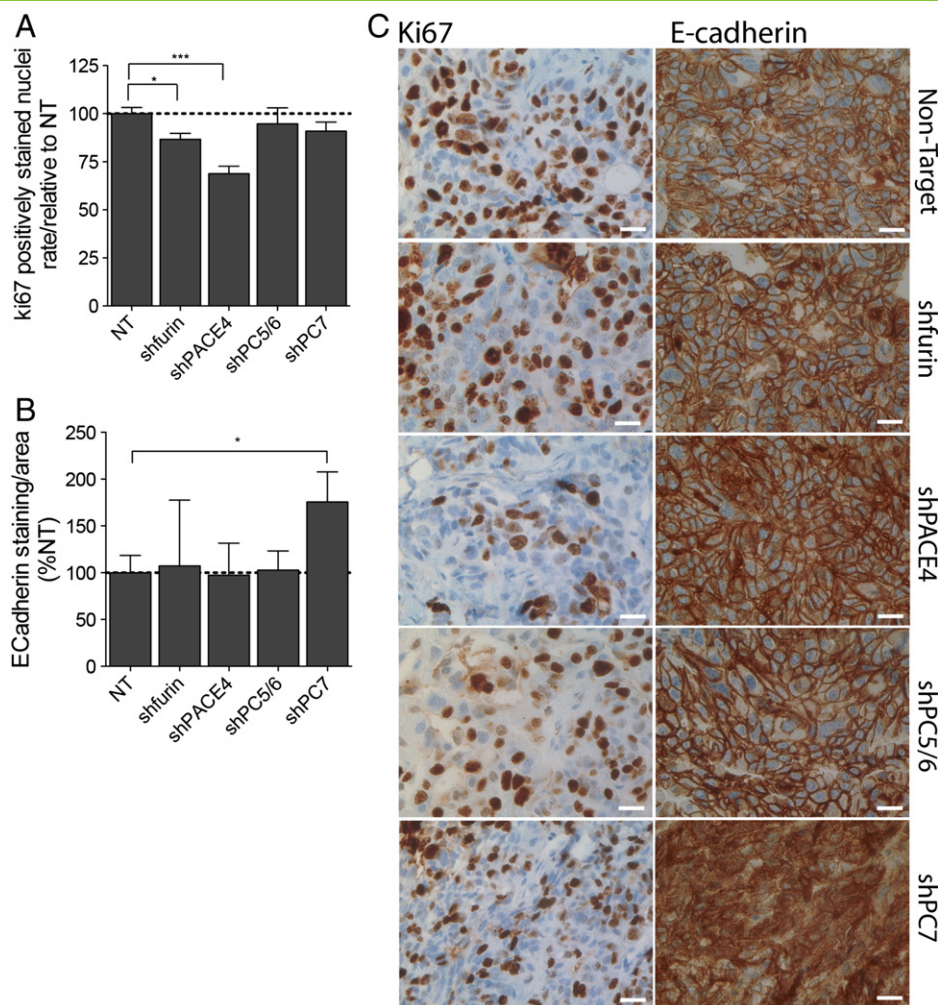
Figure 5. Xenograft IHC analyses. IHC were performed on 0.5-μm tissue sections of excised xenografts. (A) Ki67 and (B) E-cadherin immunostaining quantification using CMYK quantification in tumor areas were confirmed by hematoxylin and eosin standard counterstainings. (C) Representative fields are shown at $\times$ 400 magnification, and scale bars represent 25 μm. *P < .05 and ***P < .001.

decreased growth rate for the shPACE4 tumors, we observed a greatly increased proliferation of shPC7 tumors. Such contradictory results between *in vitro* and *in vivo* growth conditions have been reported by Couture et al. for prostate cancer cell lines [11], and these results highlight the importance of also validating *in vitro* observations in a more physiological context to take account of the conditions within the tumor microenvironment.

We also examined various biomarkers in relation to PACE4 and PC7 knockdown cell–derived xenografts. A statistically significant reduction in the Ki67 proliferation index was observed in the PACE4-silenced xenograft, supporting the observed growth phenotype. This phenomenon was in agreement with our previous report resulting in similar conclusions [11].

Evaluation of E-cadherin levels, an epithelial protein at the surface of the cells, provides a partial explanation of the surprising *in vivo* growth properties of shPC7 SKOV3 xenografts. The molecular context differentiating *in vitro* and *in vivo* assays consists not only in the growth factor availability in the animal model environment but also in the multiple cell interactions that exist in the pseudotumor that forms the xenograft. These intercellular interactions may be associated to the dramatic overgrowth of shPC7 xenografts, compared

to growth of the individual cell line *in vitro*. Intercellular interactions are partially mediated by E-cadherin that allows a Ca^{2+}-dependent homophylic interaction. E-cadherin has a dual role in the different phases of ovarian cancer metastasis [18]. It was recently shown that E-cadherin was able to promote SKOV-3 cell line overgrowth, *in vitro* [24]. In prostate cancer, E-cadherin has been proposed as a marker for tumor aggressiveness because it is re-expressed at a late stage of metastatic progression [25]. The differential *in vivo* growth of E-cadherin-positive and E-cadherin-negative DU145 prostatic cell sublines was recently evaluated. The result of this study indicated that an E-cadherin-positive xenografted cell line grows more rapidly than an E-cadherin-negative cell line [26]. In a brain tumor model, the overexpression of E-cadherin has been associated with an aggressive phenotype [27]. IHC analyses indicated increased E-cadherin levels in SKOV3 shPC7 tumors, which could partially explain the *in vivo* significantly higher growth rate of shPC7 tumors when considering the role of E-cadherin. However, the number of Ki67-positive cells remained unchanged in the shPC7 tumors compared to the control tumors. E-cadherin has been shown not to have any correlation with Ki67 for lesion classification in uterine cervical cancer [28].
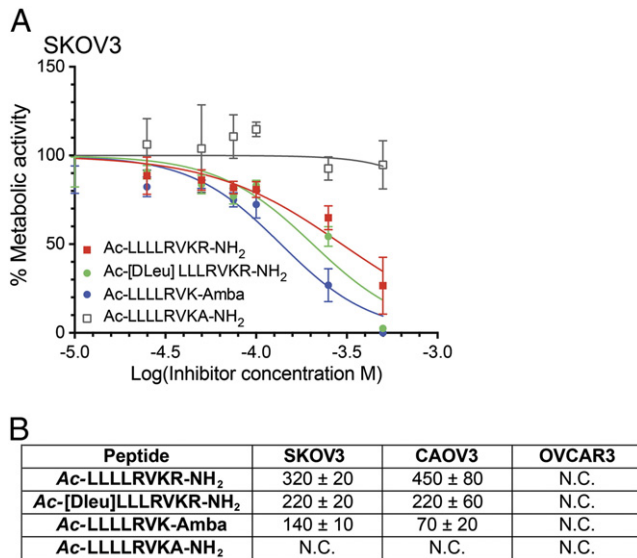
A

B

Peptide	SKOV3	CAOV3	OVCAR3
Ac-LLLLRVKR-NH$_2$	320 ± 20	450 ± 80	N.C.
Ac-[Dleu]LLLLRVKR-NH$_2$	220 ± 20	220 ± 60	N.C.
Ac-LLLLRVK-Amba	140 ± 10	70 ± 20	N.C.
Ac-LLLLRVKA-NH$_2$	N.C.	N.C.	N.C.

Figure 6. Antiproliferative activity of PACE4 inhibitors using ovarian cancer cells. (A) Dose-response growth inhibition curves of the ML peptide and its peptidomimetic analogs on SKOV3 cells are shown. (B) IC$_{50}$ of the four peptides on the PACE4-positive SKOV3 and CAOV3 cells and the PACE4-negative OVCAR3 cells is shown. Dose-response curves are representative experiments, and data in the table are means ± SEM of at least four independent experiments performed in triplicate. NC indicates that the curve did not converge at concentration below 500 μM.

PACE4 has already been highlighted for its potential role in numerous neoplasias, such as oral tongue carcinoma [29], hepatocellular carcinoma [30], glioma [31], skin cancer [32,33], and prostate cancer [7]. Whereas these studies mostly examined overexpression of PACE4, our present study focused on gene silencing as a predictive approach to define potential therapeutic benefits, as we have also recently demonstrated with prostate cancer [7,11,15]. The role of PACE4 in ovarian homeostasis has already been documented [34], and its expression has also been shown to be decreased in ovarian cancer tissues [9]. However, this latter study is in contradiction with gene expression databases such as Oncomine. This may be due to results that suggest that expression is also linked to various tumor grades [10].

As our gene silencing studies indicate that the inhibition of PACE4 might be beneficial in ovarian cancer, we then tested the application of pharmacological inhibitors of PACE4. In a recent work, we developed a peptide-based inhibitor targeting PACE4, named the ML peptide inhibitor. Using ML peptide inhibitors, we provided evidence of their effectiveness on prostate cancer cell lines [15]. These peptides were designed on the basis of the observation that PC7 prodomain-based peptides with nonpolar amino acid residues at P6 and P7 positions have better inhibition potency toward PACE4 than furin [35]. The N-terminal addition of four Leu residues to the consensus PC motif created the ML peptide (Ac-LLLLRVKR-NH$_2$). This addition allowed low nanomolar K_i to be reached (K_i = 20 nM) and provided a higher selectivity for PACE4 than for furin by up to 20- to 22-fold [15]. Our studies have shown that, on prostate cancer cell lines, such as DU145 and LNCaP, ML-peptide displays a pharmacological effect with an IC$_{50}$ in the micromolar range. In the present study, we used the PACE4-positive SKOV3 and CAOV3

cells together with the OVCAR3 cells to compare PACE4-dependent effect on cell proliferation. Again, the Ac-LLLLRVKR-NH$_2$ and its analog Ac-[DLeu]LLLLRVKR-NH$_2$ had IC$_{50}$s in the micromolar range for the PACE4-positive cells but did not display any inhibitory effect on the PACE4-negative OVCAR3 cell proliferation (Figure 6). When using the Ac-LLLLRVK-Amba peptidomimetic analogs, which display much lower K_i values (i.e., 3 nM) toward PACE4 and a higher stability profile *in vitro*, the IC$_{50}$ values lowered considerably, thus supporting a PACE4-linked effect [14]. This PACE4 dependance is also supported by a negative control peptide (Ac-LLLLRVKA-*NH$_2$*), which had no effects on proliferation of any of the tested cell lines, corroborating the notion of a PC-dependent growth inhibition as the peptide does not possess inhibitory activity toward PACE4. These key results demonstrate that pharmacological inhibition of PACE4 phenocopies the gene silencing approach and suggests new strategies for targeted therapy of ovarian cancer. This highlights the possibility of using PC-based approach to treat ovarian cancer.

The present study, along with our previous work on prostate cancer, increasingly suggests that PCs can be attractive targets for the development of novel therapies for various neoplasias. Our results offer important insights into the implication of PCs in carcinogenesis and progression of ovarian cancer. Although our results raise the hope for a major role of PACE4 in various cancer types, we cannot assume that this will be generalized to most tumor types. However, further studies with additional cancer types are now justified. Moreover, this study highlights the fact that, in opposition to prostate cancer where only PACE4 is overexpressed among the PCs, all PCs analyzed are overexpressed in ovarian cancer despite the proliferative functions being limited to PACE4. This indicates that the simple observation of overexpressed proteases, such as PCs, does not necessarily imply that it can be a pharmacological target. Validation steps that focus on inhibition rather than overexpression are clearly required.

Further studies in the fields of EOCs would also be interesting, starting with the use of other cell lines that would represent each different type of EOC. Recent studies suggest that EOC may actually initiate from a primary metastasis of müllerian tissues to develop in the ovarian environment [36,37]. Depending of the origin of the initiating cell, different affliction types may occur. Serous cancers may initiate from a tubal origin and endometrioid cancers from an endometrial origin. These two types of cancers represent the most prevalent ones and bear very different morphologic properties. It would be very relevant to discriminate whether PC implications are constant between these two types of EOC.

Finally, the determination of PACE4-specific substrates in ovarian cancer progression would pave the way to a better understanding of molecular and cellular pathways in tumorigenesis but also potentially reveal biomarkers regulated by this enzyme. Nowadays, N-terminomics methods based on mass spectrometry allow one to decipher the action of an enzyme by the characterization of its generated N-terminal fragments [38]. Evaluation of the general action of an enzyme is the crucial step to describe biologic mechanistics, and it may be of great relevance to reveal the key position of PACE4 among molecular events of ovarian cancer progression. Other mass spectrometry–based approaches for the analysis of tissues regarding the anatomic context [39–42] may also be useful for the exploration of molecular events occurring in xenografts. Indeed, it would be interesting to compare the molecular events occurring between the developed tissue and the surrounding environment or within the

tissue itself between the different interacting cell types, for example, between blood vessels and the cancerous cells.

In conclusion, the present study provides a new outlook for the use of PACE4 inhibitors in neoplastic afflictions.

Acknowledgments

References

[1] Longuespée R, Boyon C, Desmons A, Vinatier D, Leblanc E, Farré I, Wisztorski M, Ly K, D'Anjou F, and Day R, et al (2012). Ovarian cancer molecular pathology. *Cancer Metastasis Rev* **31**, 713–732.

[2] Khatib AM, Siegfried G, Chrétien M, Metrakos P, and Seidah NG (2002). Proprotein convertases in tumor progression and malignancy: novel targets in cancer therapy. *Am J Pathol* **160**, 1921–1935.

[3] Couture F, D'Anjou F, and Day R (2011). On the cutting edge of proprotein convertase pharmacology: from molecular concepts to clinical applications. *Biomol Concepts* **2**, 421–438.

[4] Fugère M and Day R (2005). Cutting back on pro-protein convertases: the latest approaches to pharmacological inhibition. *Trends Pharmacol Sci* **26**, 294–301.

[5] Cheng M, Watson PH, Paterson JA, Seidah N, Chrétien M, and Shiu RP (1997). Pro-protein convertase gene expression in human breast cancer. *Int J Cancer* **71**, 966–971.

[6] Bassi DE, Mahloogi H, Al-Saleem L, Lopez De Cicco R, Ridge JA, and Klein-Szanto AJ (2001). Elevated furin expression in aggressive human head and neck tumors and tumor cell lines. *Mol Carcinog* **31**, 224–232.

[7] D'Anjou F, Routhier S, Perreault JP, Latil A, Bonnel D, Fournier I, Salzet M, and Day R (2011). Molecular validation of PACE4 as a target in prostate cancer. *Transl Oncol* **4**, 157–172.

[8] Juliano RL and Haskill S (1993). Signal transduction from the extracellular matrix. *J Cell Biol* **120**, 577–585.

[9] Fu Y, Campbell EJ, Shepherd TG, and Nachtigal MW (2003). Epigenetic regulation of proprotein convertase PACE4 gene expression in human ovarian cancer cells. *Mol Cancer Res* **1**, 569–576.

[10] Page RE, Klein-Szanto AJ, Litwin S, Nicolas E, Al-Jumaily R, Alexander P, Godwin AK, Ross EA, Schilder RJ, and Bassi DE (2007). Increased expression of the pro-protein convertase furin predicts decreased survival in ovarian cancer. *Cell Oncol* **29**, 289–299.

[11] Couture F, D'Anjou F, Desjardins R, Boudreau F, and Day R (2012). Role of proprotein convertases in prostate cancer progression. *Neoplasia* **14**, 1032–1042.

[12] D'Anjou F, Couture F, Desjardins R, and Day R (2014). Knockdown strategies for the study of proprotein convertases and proliferation in prostate cancer cells. *Methods Mol Biol* **1103**, 67–82.

[13] Pham NA, Morrison A, Schwock J, Aviel-Ronen S, Iakovlev V, Tsao MS, Ho J, and Hedley DW (2007). Quantitative image analysis of immunohistochemical stains using a CMYK color model. *Diagn Pathol* **2**, 8.

[14] Kwiatkowska A, Couture F, Levesque C, Ly K, Desjardins R, Beauchemin S, Prahl A, Lammek B, Neugebauer W, and Dory YL, et al (2014). Design, synthesis, and structure–activity relationship studies of a potent PACE4 inhibitor. *J Med Chem* **57**, 98–109.

[15] Levesque C, Fugère M, Kwiatkowska A, Couture F, Desjardins R, Routhier S, Moussette P, Prahl A, Lammek B, and Appel JR, et al (2012). The Multi-Leu peptide inhibitor discriminates between PACE4 and furin and exhibits antiproliferative effects on prostate cancer cells. *J Med Chem* **55**, 10501–10511.

[16] Roehm NW, Rodgers GH, Hatfield SM, and Glasebrook AL (1991). An improved colorimetric assay for cell proliferation and viability utilizing the tetrazolium salt XTT. *J Immunol Methods* **142**, 257–265.

[17] Vollenweider F, Benjannet S, Decroly E, Savaria D, Lazure C, Thomas G, Chrétien M, and Seidah NG (1996). Comparative cellular processing of the human immunodeficiency virus (HIV-1) envelope glycoprotein gp160 by the mammalian subtilisin/kexin-like convertases. *Biochem J* **314**, 521–532.

[18] Sundfeldt K (2003). Cell-cell adhesion in the normal ovary and ovarian tumors of epithelial origin; an exception to the rule. *Mol Cell Endocrinol* **202**, 89–96.

[19] Sawada K, Mitra AK, Radjabi AR, Bhaskar V, Kistner EO, Tretiakova M, Jagadeeswaran S, Montag A, Becker A, and Kenny HA (2008). Loss of E-cadherin promotes ovarian cancer metastasis via α5-integrin, which is a therapeutic target. *Cancer Res* **68**, 2329–2339.

[20] Siegel R, Naishadham D, and Jemal A (2013). Cancer statistics, 2013. *CA Cancer J Clin* **63**, 11–30.

[21] Ferlay J, Steliarova-Foucher E, Lortet-Tieulent J, Rosso S, Coebergh JW, Comber H, Forman D, and Bray F (2013). Cancer incidence and mortality patterns in Europe: estimates for 40 countries in 2012. *Eur J Cancer* **49**, 1374–1403.

[22] Lindert AC, Barents JW, and Pinedo HM (1978). The silent killer: treatment of a patient by the oncological team. *Ned Tijdschr Geneeskd* **122**, 65–68.

[23] Seidah NG and Prat A (2012). The biology and therapeutic targeting of the proprotein convertases. *Nat Rev Drug Discov* **11**, 367–383.

[24] Dong LL, Liu L, Ma CH, Li JS, Du C, Xu S, Han LH, Li L, and Wang XW (2012). E-cadherin promotes proliferation of human ovarian cancer cells *in vitro* via activating MEK/ERK pathway. *Acta Pharmacol Sin* **33**, 817–822.

[25] De Marzo AM, Knudsen B, Chan-Tack K, and Epstein JI (1999). E-cadherin expression as a marker of tumor aggressiveness in routinely processed radical prostatectomy specimens. *Urology* **53**, 707–713.

[26] Putzke AP, Ventura AP, Bailey AM, Akture C, Opoku-Ansah J, Celiktaş M, Hwang MS, Darling DS, Coleman IM, and Nelson PS, et al (2011). Metastatic progression of prostate cancer and e-cadherin: regulation by Zeb1 and Src family kinases. *Am J Pathol* **179**, 400–410.

[27] Lewis-Tuffin LJ, Rodriguez F, Giannini C, Scheithauer B, Necela BM, Sarkaria JN, and Anastasiadis PZ (2010). Misregulated E-cadherin expression associated with an aggressive brain tumor phenotype. *PLoS One* **5**, e13665.

[28] Samir R, Asplund A, Tot T, Pekar G, and Hellberg D (2011). High-risk HPV infection and CIN grade correlates to the expression of c-myc, CD4+, FHIT, E-cadherin, Ki-67, and p16INK4a. *J Low Genit Tract Dis* **15**, 280–286.

[29] Estilo CL, O-charoenrat P, Talbot S, Socci ND, Carlson DL, Ghossein R, Williams T, Yonekawa Y, Ramanathan Y, and Boyle JO, et al (2009). Oral tongue cancer gene expression profiling: identification of novel potential prognosticators by oligonucleotide microarray analysis. *BMC Cancer* **9**, 11.

[30] Kurokawa Y, Matoba R, Nakamori S, Takemasa I, Nagano H, Dono K, Umeshita K, Sakon M, Monden M, and Kato K (2004). PCR-array gene expression profiling of hepatocellular carcinoma. *J Exp Clin Cancer Res* **23**, 135–141.

[31] Delic S, Lottmann N, Jetschke K, Reifenberger G, and Riemenschneider MJ (2012). Identification and functional validation of *CDH11*, *PCSK6* and *SH3GL3* as novel glioma invasion-associated candidate genes. *Neuropathol Appl Neurobiol* **38**, 201–212.

[32] Bassi DE, Lopez De Cicco R, Cenna J, Litwin S, Cukierman E, and Klein-Szanto AJ (2005). PACE4 expression in mouse basal keratinocytes results in basement membrane disruption and acceleration of tumor progression. *Cancer Res* **65**, 7310–7319.

[33] Mahloogi H, Bassi DE, and Klein-Szanto AJ (2002). Malignant conversion of non-tumorigenic murine skin keratinocytes overexpressing PACE4. *Carcinogenesis* **23**, 565–572.

[34] Mujoomdar ML, Hogan LM, Parlow AF, and Nachtigal MW (2011). *Pcsk6* mutant mice exhibit progressive loss of ovarian function, altered gene expression, and formation of ovarian pathology. *Reproduction* **141**, 343–355.

[35] Fugère M and Day R (2002). Inhibitors of the subtilase-like pro-protein convertases (SPCs). *Curr Pharm Des* **8**, 549–562.

[36] Kurman RJ and Shih Ie M (2010). The origin and pathogenesis of epithelial ovarian cancer: a proposed unifying theory. *Am J Surg Pathol* **34**, 433–443.

[37] Longuespée R, Gagnon H, Boyon C, Strupat K, Dauly C, Kerdraon O, Ighodaro A, Desmons A, Dupuis J, and Wisztorski M, et al (2013). Proteomic analyses of serous and endometrioid epithelial ovarian cancers – cases studies – molecular insights of a possible histological etiology of serous ovarian cancer. *Proteomics Clin Appl* **7**, 337–354.

[38] Kleifeld O, Doucet A, auf dem Keller U, Prudova A, Schilling O, Kainthan RK, Starr AE, Foster LJ, Kizhakkedathu JN, and Overall CM (2010). Isotopic labeling of terminal amines in complex samples identifies protein N-termini and protease cleavage products. *Nat Biotechnol* **28**, 281–288.

[39] El Ayed M, Bonnel D, Longuespée R, Castelier C, Franck J, Vergara D, Desmons A, Tasiemski A, Kenani A, and Vinatier D, et al (2010). MALDI imaging mass spectrometry in ovarian cancer for tracking, identifying, and validating biomarkers. *Med Sci Monit* **16**, BR233–245.

[40] Calligaris D, Longuespée R, Debois D, Asakawa D, Turtoi A, Castronovo V, Noël A, Bertrand V, De Pauw-Gillet MC, and De Pauw E (2013). Selected protein monitoring in histological sections by targeted MALDI-FTICR in-source decay imaging. *Anal Chem* **85**, 2117–2126.

[41] Longuespée R, Boyon C, Castellier C, Jacquet A, Desmons A, Kerdraon O, Vinatier D, Fournier I, Day R, and Salzet M (2012). The C-terminal fragment of

the immunoproteasome PA28S (Reg alpha) as an early diagnosis and tumor-relapse biomarker: evidence from mass spectrometry profiling. *Histochem Cell Biol* **138**, 141–154.

[42] Franck J, Longuespée R, Wisztorski M, Van Remoortere A, Van Zeijl R, Deelder A, Salzet M, McDonnell L, and Fournier I (2010). MALDI mass spectrometry imaging of proteins exceeding 30,000 daltons. *Med Sci Monit* **16**, BR293–99.